Marshall JS, Palmer WKM. 1948. The distribution of raindrops with size. *J. Meteorol.* **5**: 165–166.

Marshall JS, Hitschfeld W, Gunn KLS. 1955. Advances in radar weather. *Adv. Geophys.* **2**: 1–56.

Met Office. 2009. Fact sheet number 15: radar. National Meteorological Library and Archive. http://www.metoffice.gov.uk/learning/library/publications/factsheets (accessed 15 December 2013).

Nesbitt SW, Anders AM. 2009. Very high resolution precipitation climatologies from the Tropical Rainfall Measuring Mission precipitation radar. *Geophys. Res. Lett.* **36**: *L15815*.

Overeem A, Holleman I, Buishand A. 2009. Derivation of a 10-year radar-based climatology of rainfall. *J. Appl. Meteorol. Climatol.* **48**: 1448–1463.

Parkes BL, Wetterhall F, Pappenberger F *et al.* 2013. Assessment of a 1-hour gridded precipitation dataset to drive a hydrological model: a case study of the summer 2007 floods in the Upper Severn, UK. *Hydrol. Res.* **44**(1): 89–105.

Rutledge SA, Hobbs PV. 1983. The mesoscale and microscale structure and organization of clouds and precipitation in midlatitude cyclones. VIII: a model for the 'Seeder–Feeder' process in warm frontal rainbands. *J. Atmos. Sci.* **40**: 1185–1206.

Smith A, Lott N, Vose R. 2011. The integrated surface database: recent developments and partnerships. *Bull. Am. Meteorol. Soc.* **92**: 704–708.

Smyth TJ, Illingworth AJ. 1998. Radar estimates of rainfall rates at the ground in bright band and non-bright band events. *Q. J. R. Meteorol. Soc.* **124**: 2417–2434.

Tabary P, Dupuy P, L'Henaff G *et al.* 2012. A 10-year (1997–2006) reanalysis of quantitative precipitation estimation over France: methodology and first results, in *Weather Radar and Hydrology (Proceedings of a Symposium held in Exeter, UK, April 2011)*, Publication 351. IAHS: Wallingford, UK, pp 255–260.

Warren RA, Kirshbaum DJ, Plant RS *et al.* 2014. A 'Boscastle-type' quasi-stationary convective system over the UK Southwest peninsula. *Q. J. R. Meteorol. Soc.* **140**: 240–257.

Correspondence to: Jonathan G. Fairman Jr

jonathan.fairman@manchester.ac.uk

doi:10.1002/wea.2486

Atmospheric divergence over equatorial East Africa and its influence on distribution of rainfall

Kiprop Vincent Koech

Department of Meteorology, University of Nairobi, Kenya

Introduction

In East Africa, rainfall amounts and distribution are the most important factors governing crop yields (Muti and Kibe, 2009). Since most food production systems over the region are mainly rain-fed, weather forecasts are crucial. Therefore, this analysis focuses on divergence of the atmospheric flow with the aim of contributing to the understanding of regional weather.

The idea that surface convergence and rainfall are related is not new. Marshall *et al.* (2001) found that initial rainfall morphology is related not only to the amount of low-level convergence but to the depth of the convergence. Convergence is the piling up of air above a region, whereas divergence is the spreading of air above some region (Ahrens, 2011). Convergence and divergence of air may result from changes in wind speed or wind direction (Ahrens, 2011). In addition, convergence may be due to frictionally driven, cross-isobaric flow (Zehnder, 2001).

Area of study

The area under the focus of this analysis is equatorial East Africa (Figure 1). Twenty-one stations have been selected to represent the region, based on homogeneous rainfall zones.

East Africa experiences two climatological rainy seasons. During southern hemisphere summer, the weather of equatorial East Africa is influenced by the northeast monsoon. During northern hemisphere summer, the region is under the influence of the southeast monsoon. The southeast monsoon is cool, moist and shallow, and is generally associated with cool, cloudy and dry conditions over the region (Christian *et al.*, 2011).

Data

Two datasets were used in the analysis. These are monthly mean rainfall and divergence data for the period 1979–2008. The rainfall data were obtained from the National Oceanic and Atmospheric Administration (NOAA) Climate Prediction Centre (CPC). The spatial resolution of the CPC dataset is 0.5° × 0.5°. Divergence data were obtained from European Centre for Medium Range Weather Forecasting (ECMWF) ERA-Interim dataset. The spatial resolution of the ECMWF dataset is 0.125° × 0.125°.

Seasonal variation of upper tropospheric divergence

As atmospheric sounding and instability indices reveal, most of the tropical zone is essentially convective, although variations occur on diurnal, latitudinal, and seasonal scales, as well as with altitude (Galvin, 2008). In this section, we focus on the seasonal variation of upper tropospheric divergence over the region. The seasonal variation is based on the monthly mean for the period 1979–2008.

The seasonal march of upper tropospheric divergence has a bimodal pattern (Figure 2). During March-April-May (MAM) and October-November-December (OND), there is peak upper level divergence at 300 and 200hPa over the region. During

MAM there is a relatively higher peak in upper level divergence compared with the peak divergence in OND. This implies that convective activity during MAM season is deeper compared with the OND season. This leads to the relatively high rainfall peak that is observed in MAM (Figure 2). These peaks are associated with the presence of the Intertropical Convergence Zone (ITCZ) over the region.

During June-July-August (JJA), there is peak upper level convergence over the region at 300 and 200hPa. The upper level convergence during JJA can be attributed to the prevailing wind. During JJA, East Africa is under the influence of the southeast monsoon. The southeast monsoon is fairly moist, diffluent and has a subsiding nature (Opijah *et al*., 2008). Due to the diffluence at the lower troposphere, upper level divergence must occur.

The subsidence that occurs during JJA has two effects. The first is that vertical air motion is either curtailed or is confined to the lower troposphere over the region. Consequently, stratified clouds such as stratus and stratocumulus are formed, leading to overcast skies, foggy conditions and drizzle. This large-scale subsidence is the major factor in the origin and maintenance of the trade winds inversion (Sarah and David, 2012). The second effect of this subsidence is that it weakens disturbances and troughs over the region during JJA.

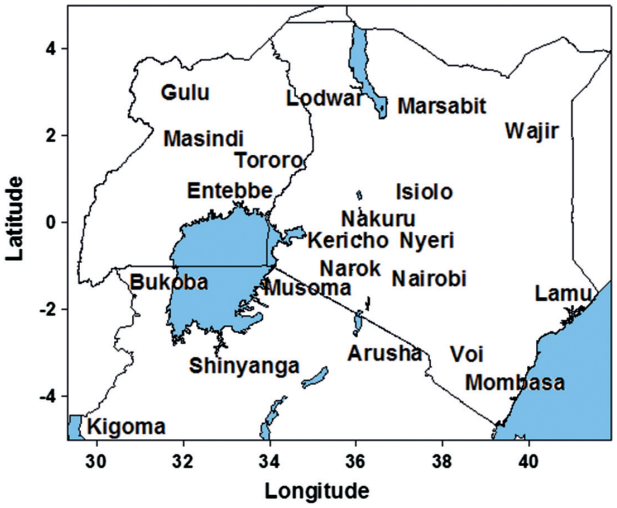

Figure 1. Map of equatorial East Africa, showing the area under study and the rainfall stations whose data were used. The rainfall stations were selected based on homogeneous rainfall zones in the region. as developed by Indeje et al. (2000).

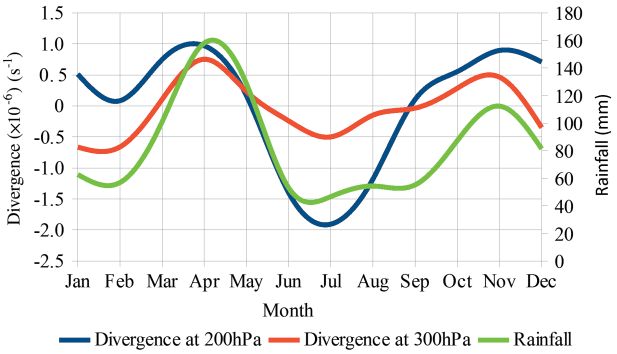

Figure 2. Seasonal march of upper tropospheric divergence and rainfall over equatorial East Africa. The seasonal march is based on the long term mean (1979–2008) over 21 stations. The seasonal cycle of the divergence is bimodal. Peak divergence occurs during March-April-May (MAM) and October-November-December (OND) with peak divergence during MAM being higher than the peak divergence during OND.

Diurnal variation of tropospheric divergence

Three types of diurnal cycle in tropical precipitation can be identified, according to Kikuchi and Wang (2008). These are: oceanic, continental, and coastal diurnal cycles of tropical precipitation (Kikuchi and Wang, 2008). In this section, we will focus on identifying only the coastal and the continental diurnal regimes in the upper tropospheric divergence.

In order to determine the diurnal regime over the regional coastal strip, upper level divergence was analysed over Lamu and Mombasa. To identify the continental type, the diurnal pattern over the Lake Victoria basin was analysed over seven stations, namely: Gulu, Masindi, Tororo, Entebbe, Kericho, Bukoba and Musoma.

Over the Lake Victoria basin (Figure 3), the diurnal march of upper level divergence has a peak in the afternoon (1200 UTC). The diffluent upper tropospheric flow at 1200 UTC favours the development and intensification of the Mesoscale Convective Systems (MCSs) that are observed over the basin. The convective weather systems will dissipate towards 1800 UTC as upper level divergence decreases in magnitude.

The diurnal cycle in divergence over the basin is a result of the diurnal cycle of solar radiation. Heating of the surface during the day provides buoyant energy that mixes the near-surface air and generates rising thermals (Gordon, 2008). Due to the rising thermals, a surface heat low is generated which favours low level convergence and ascending air motion. From considerations of conservation of mass, divergence must occur in the upper levels to compensate for accumulation of mass due to the rising thermals.

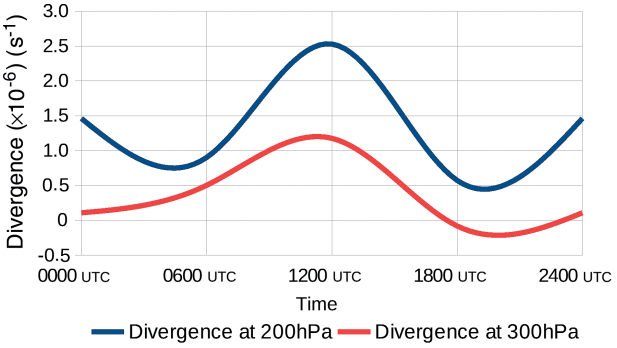

Figure 3. Diurnal march of upper tropospheric divergence over the Lake Victoria basin based on the long term mean (1979–2008) of divergence at synoptic hours. Peak divergence is observed at 1200 UTC.

The diurnal cycle of upper tropospheric divergence for the regional coastal strip is shown in Figure 4. This pattern in upper level divergence favours occurrence of rainfall at night and in the early morning. The upper level convergence over the coast has economic implications in that it ensures that the coastal sky is clear of clouds and convective systems during daytime.

Spatial distribution plots

In this section, the distribution of divergence over the region is presented at 850 and 300hPa. The spatial plots are based on the long term mean of divergence over the study period.

In the lower troposphere (850hPa), convergence is observed over the convectively active areas of East Africa (Figure 5). These areas are Uganda, northwestern Tanzania, highlands west of the Rift Valley (places such as Kericho, Kisii, Kakamega and Mt. Elgon) and a few places over central Kenya (the Mt. Kenya region and the Aberdare Range).

The arid and semi-arid areas of the region experience divergence at 850hPa (Figure 5). These areas include the southeastern lowlands of Kenya (Kitui, Voi and Tsavo), northern and eastern parts of Kenya (Mandera, Turkana, Dadaab and Garissa) and several parts of northern Tanzania. The low level divergence over these areas leads to subsidence which inhibits convection from taking place. The subsiding air warms dry adiabatically and contributes to clear skies. Thus, in addition to the dry conditions that are observed over these areas, relatively high temperatures are also observed due to the warm subsiding air and the resulting clear skies.

The dominance of the mesoscale features can be identified at 850hPa (Figure 5). For example, over the Lake Victoria basin, the land-lake breeze circulation is evident. Over the adjacent highlands such as Kisii, Kericho and Kakamega, there is low level convergence, while over the lake there is divergence at 850hPa.

The tracks of the East Africa Low Level Jet (EALLJ) and the Turkana Jet can be mapped out based on the divergence at 850hPa (Figure 5). The tracks of the low level jet streams are identified as zones of low level divergence at 850hPa over northern and northeastern Kenya. The low level divergence over these areas is as a result of acceleration of air parcels within the jet streams. As the air parcels accelerate they spread out, leading to divergence at 850hPa.

In the upper troposphere (300hPa), a mirror image of the pattern in the lower troposphere is observed (Figure 6). This mirror image sustains the pattern at low levels by ensuring that there is continuity of mass. For example, over most parts of the highlands west of Rift Valley, northwestern Tanzania and several places in Uganda, there is upper level divergence. Over arid and semi-arid areas such as northeastern Tanzania, northern Kenya and the southeastern lowlands of Kenya, there is upper level convergence at 300hPa (Figure 6).

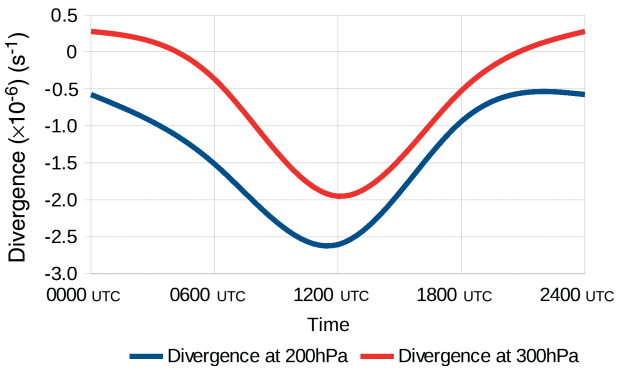

Figure 4. Diurnal march of upper tropospheric divergence over the regional coastal strip of equatorial East Africa. Peak convergence is observed at 1200 UTC while divergence is observed at night and early morning at 300hPa.

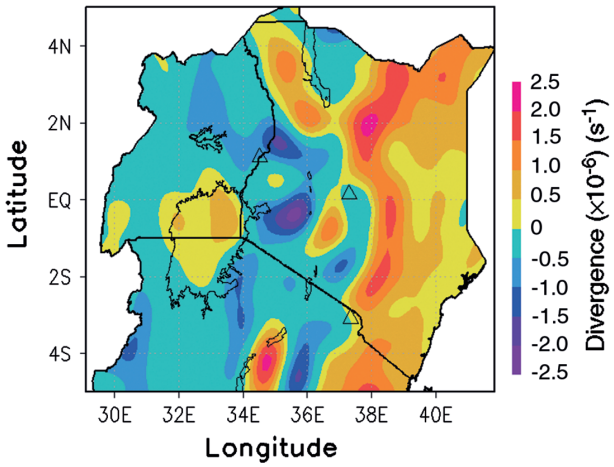

Figure 5. Spatial distribution of long term mean of divergence at 850hPa over equatorial East Africa. Blue and purple shading represents areas of convergence while yellow, brown and red shading represents areas of divergence.

Spectral analysis

In this section we focus on variability on the interannual time scale. Our interest is in the systems that account for most of the variance in the observed divergence in the upper troposphere. Since the tropical atmosphere is moist up to between 300 and 200hPa (Carrillo and Raymond, 2005), our highest pressure level of interest is 200hPa.

In order to detect interannual variations, Fourier series analysis was used. Fourier series is an appropriate representation due to its ability to successfully model waves in the atmosphere, as well as phenomena resulting from solar forcing (Duchon and Hale, 2012). Fourier series decomposes a dataset into harmonics (sinusoidal waveforms) such that when all harmonics are added together they produce the time series (Duchon and Hale, 2012). The variance at each harmonic frequency is given by the square of its amplitude divided by 30, except at the last harmonic (Duchon and Hale, 2012).

Fourier Series Analysis takes the form shown in Equation 1.

$$\mathbf{y} = \bar{\mathbf{y}} + \sum_{j=1}^{j=h}\left(\boldsymbol{a}_j \cos\frac{2\pi ij}{N} + \boldsymbol{b}_j \sin\frac{2\pi ij}{N}\right) \quad (1)$$

In Equation 1:

N is the number of years. In this case $N = 30$ h = N/2. Therefore, in this case, h = 15.

j represents the individual harmonic.

i is the number of observations. $i = 1, 2, 3, \ldots, N$

$\bar{y}$ is the mean of the time series.

Figure 7 is a periodogram of the different harmonics in divergence at 200hPa. A periodogram is a plot of variance associated with each harmonic versus the harmonic number (Duchon and Hale, 2012). From Figure 7, the oscillation that accounts for most of the variance is the second harmonic. This second harmonic has a period of 11 years (Figure 8) which closely corresponds to the sunspot cycle (Figure 9).

Based on the second harmonic (Figure 8), peak divergence at 200hPa occurred in 1989/1990 and 2000. During these years (Figure 9), sunspot maxima were recorded. In the 11-year cycle, changes in upper level divergence are such that there is an increase in intensity of upper level divergence during sunspot maxima followed by a decrease in intensity during sunspot minima.

Large scale air pressure gradients are the main factors whose variations can be tied to the sunspot cycle: gradients are large during sunspot maxima and small during sunspot minima (Wefer, 2002). Steep pressure gradients imply strong winds, and weak pressure gradients, light winds (Ahrens, 2011). A study related to stratospheric heating by

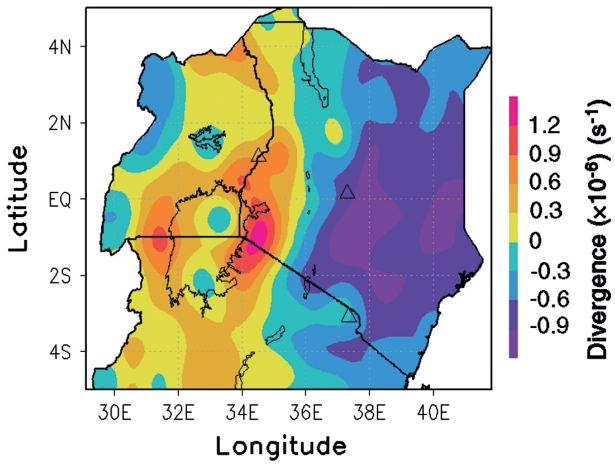

Figure 6. Spatial distribution of long term mean of divergence at 300hPa over equatorial East Africa. Blue and purple shading represents areas of convergence while yellow, brown and red shading represents areas of divergence.

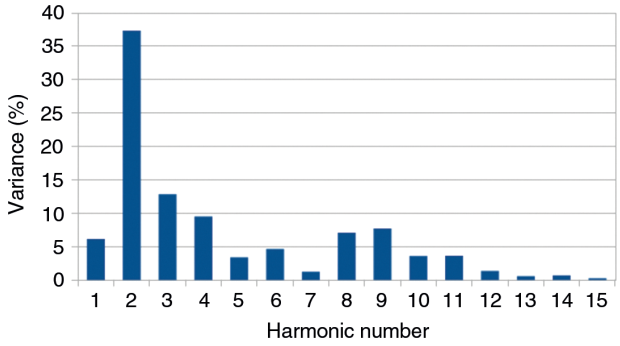

Figure 7. Periodogram of different harmonics in the observed divergence at 200hPa over 21 stations in equatorial East Africa. The second harmonic accounts for most of the variance at 35%. There is an indication of presence of oscillatory systems with higher frequency of variability.

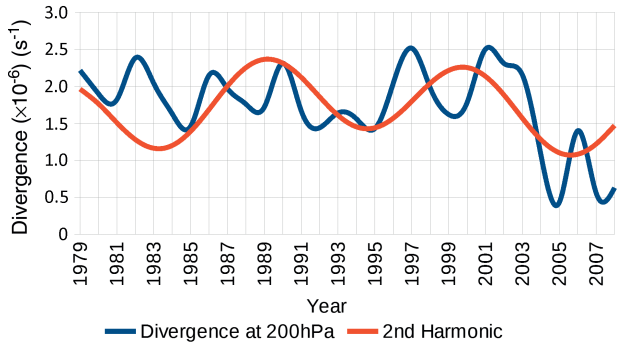

Figure 8. Plot of the second harmonic in the upper tropospheric divergence over equatorial East Africa.

Haigh (1996) tends to be in agreement with this approach, which is based on pressure gradients. At solar maximum, a warming of the summer stratosphere was found to strengthen the easterly winds, which penetrated more into the equatorial upper troposphere, causing the tropical Hadley circulations to broaden (Haigh, 1996).

Based on the harmonics in the annual mean (Figure 7), there is an indication of the presence of oscillatory systems with a higher frequency of variability. We therefore seek to identify whether there is any signature of the El Niño Southern Oscillation in the upper tropospheric divergence. The 4- to 6-year periodicity has been associated with the El Niño Southern Oscillation, which has an influence on the Walker Circulation, as hypothesized by Bjerknes (1969). The Walker Circulation is weak in March and April (Philander, 1990). Therefore, in order to detect the influence of the El Niño Southern Oscillation, spectral analysis was performed on divergence at 200hPa for the OND season.

The results of the spectral analysis are shown in Figures 10 and 11. In Figure 10, apart from the fundamental harmonic, the sixth harmonic accounts for most of the variance. The sixth harmonic and the eighth harmonic have a periodicity that ranges from 4 to 5 years (Figure 11).

The sixth and the eighth harmonic tend to provide a close fit to the observed time series (Figure 11). Based on the sixth and the eighth harmonic, the years with marked upper tropospheric divergence are 1997/1998 and 2002/2003. These are some of the years when there was a strong El Niño over the region.

During El Niño there is anomalous weakening of the trade winds (Bjerknes, 1969) and there is an eastward shift in the Walker Circulation (Philander, 1990). This eastward shift favours the invasion of the quasi-permanent low pressure systems that sit over the Congo basin to the East African region. This invasion leads to large scale low level convergence over East Africa. The weak trade winds favour the meridional arm of the ITCZ to sit over vast swaths of East Africa during an El Niño year.

The El Niño also affects the zonal arm of the ITCZ over the region. This is because during El Niño, convective zones over the southwestern Indian Ocean and adjacent land are displaced equatorward (Philander, 1990). As a result, El Niño brings enhanced rainfall to equatorial East Africa but diminished rainfall to southeastern Africa (Philander, 1990).

The amplitudes of the sixth and eighth harmonics (Figure 11) vary, and this causes the effects of the harmonics on the observed weather to vary over time. Due to the periodic nature of El Niño Southern Oscillation, the harmonics in the upper tropospheric divergence can be extrapolated to determine when an El Niño will occur. However, as stated by Philander (1990), such a model is too crude to predict what amplitude the El Niño will attain.

Some of the years with marked upper level divergence are 1996/1997, 1999/2000 and 2004/2005 (Figure 11). During these La Niña years, Kenya experienced drought. The trade winds are intense during La Niña (Philander, 1990). The intense trade winds confine the convective systems that are embedded in the meridional arm of the ITCZ to the western parts of the region.

Conclusions

Over the arid and semi-arid areas of equatorial East Africa, divergence is observed at the low levels and convergence at the high levels of the troposphere. Over convectively active areas such as the highlands of the Lake Victoria basin, there is low level convergence and upper level divergence.

Local features play an important role in contributing to the nature of divergence of air flow as evident over the Lake Victoria basin and northeastern Kenya. Over areas with generally flat topography, such as northeastern Kenya and southeastern

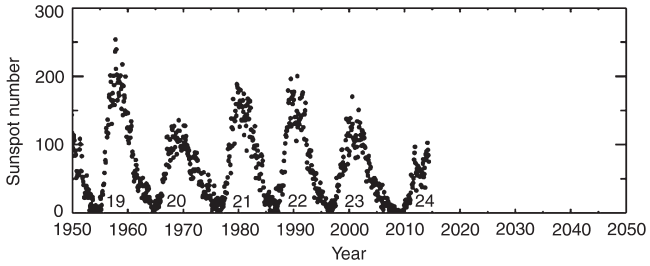

Figure 9. Monthly averaged sunspot numbers, NASA (2014). Sunspot maxima were recorded in 1960, 1970, 1980, 1990 and 2000.

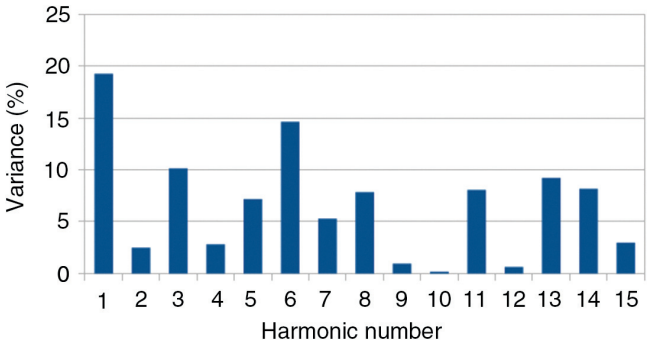

Figure 10. A periodogram of harmonics in the seasonal long term mean of divergence at 200hPa for October-November-December. Apart from the first (fundamental) harmonic, the sixth harmonic accounts for most of the variance.

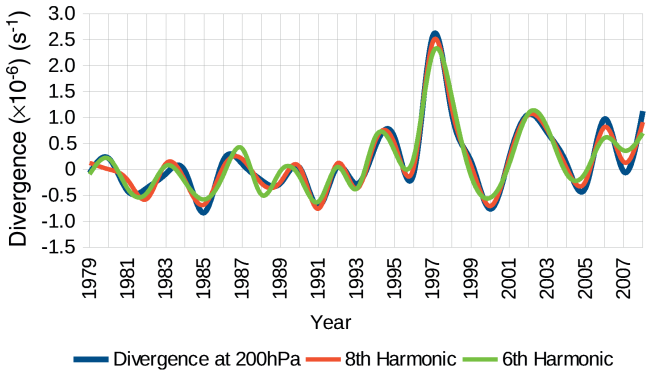

Figure 11. A plot of harmonics with a periodicity of 4–5 years in the upper tropospheric divergence at 200hPa for October-November-December.

lowlands of Kenya, the role of topography is minimal and low level divergence is observed.

Upper tropospheric divergence varies seasonally over equatorial East Africa. The seasonal variation is bimodal with peak divergence during MAM and OND at 300 and 200hPa. These peaks are associated with the presence of ITCZ over the region. During JJA, there is upper tropospheric convergence over the region due to the trade winds inversion.

Upper tropospheric divergence exhibits diurnal variability over the region. Over the regional coastal strip, upper tropospheric divergence occurs during the night, with peaks in the late night and early morning at 300hPa. The continental areas (Lake Victoria basin) experience peak upper tropospheric divergence in the afternoon.

The upper tropospheric divergence over the region exhibits interannual variability. These variations can be detected by means of spectral analysis and can be modelled using the resulting harmonics.

The El Niño Southern Oscillation has an influence on upper tropospheric divergence over the region. During El Niño, there is an increase in the intensity of upper tropospheric divergence over the region.

Acknowledgement

The author thanks Dr. Franklin Opijah, PhD - senior lecturer at the University of Nairobi Department of Meteorology - for the sincere guidance right from the formative stages of this article. The author also appreciates the assistance of this journal's editorial team.

References

Ahrens CD. 2011. *Essentials of Meteorology: An Invitation to the Atmosphere*. Cengage Learning: Belmont, CA.

Bjerknes J. 1969. Atmospheric teleconnections from the equatorial Pacific 1. *Mon. Weather Rev.* **97**(3): 163–172.

Carrillo LC, Raymond DJ. 2005. Moisture tendency equations in a tropical atmosphere. *J. Atmos. Sci.* **62**(5): 1601–1613.

Christian W, Gerald HH, Axal T *et al.* 2011. Reduced interannual rainfall variability in East Africa during the last ice age. *Science* **333**: 743–747.

Duchon C, Hale R. 2012. *Time Series Analysis in Meteorology and Climatology: An Introduction*, Volume 7. John Wiley & Sons: Chichester, UK.

Galvin JFP. 2008. The weather and climate of the tropics Part 3–Synoptic-scale weather systems. *Weather* **63**(1): 16–22.

Gordon BB. 2008. *Ecological Climatology: Concepts and Applications*, 2nd Edition. Cambridge University Press: Cambridge, UK and New York, NY.

Haigh JD. 1996. The impact of solar variability on climate. *Science* **272**(5264): 981–984.

Indeje M, Semazzi FH, Ogallo LJ. 2000. ENSO signals in East African rainfall seasons. *Int. J. Clim.* **20**(1): 19–46.

Kikuchi K, Wang B. 2008. Diurnal precipitation regimes in the global tropics*. *J. Clim.* **21**(11): 2680–2696.

Marshall JS, Brad SF, Peter SR. 2001. Rainfall morphology in Florida convergence zones: a numerical study. *Mon. Weather Rev.* **129**: 177–197.

Muti SM, Kibe AM. 2009. The effects of East African low level jet on food security in horn of Africa: a case study of coastal region of Kenya. *Afr. J. Food Agric. Nutr. Dev.* **9**(8): 1761–1777.

NASA. 2014. Monthly averaged sunspot numbers. http://solarscience.msfc.nasa.gov/images/Zurich_Color_Small.jpg (accessed 7 July 2014).

Opijah FJ, Ng'ang'a JK, Omedo G *et al.* 2008. Contribution to the heat budget in Nairobi metro-area by the anthropogenic heat component. *J. Kenya Meteorol. Soc.* **2**(1): 53–64.

Philander SGH. 1990. *El Niño, La Niña and the El Niño Southern Oscillation*. Academic Press: San Diego, CA.

Sarah EM, David JN. (eds) 2012. *Quaternary environmental change in the tropics*. John Wiley & Sons: Chichester, UK.

Wefer G. (ed.) 2002. *Climate Development and History of the North Atlantic Realm*. Springer: Philadelphia, PA and New York, NY.

Zehnder JA. 2001. A comparison of convergence-and surface-flux-based convective parameterizations with applications to tropical cyclogenesis. *J. Atmos. Sci.* **58**(3): 283–301.

Correspondence to: Kiprop Vincent Koech
koechkiprop@ymail.com

doi:10.1002/wea.2447